academicJournals

Vol. 8(25), pp. 1362-1370, 9 July, 2013
DOI: 10.5897/IJPS2013.3942
ISSN 1992 - 1950 © 2013 Academic Journals
http://www.academicjournals.org/IJPS

International Journal of Physical Sciences

Full Length Research Paper

Experimental study of air-water turbulent flow structures on stepped spillways

Mohammad Reza Beheshti[1]*, Amir Khosrojerdi[1] and Seyed Mahmud Borghei[2]

[1]Department of Water Science and Engineering, Science and Research Branch, Islamic Azad University, Tehran, Iran.
[2]Department of Civil Engineering, Sharif University of Technology, Tehran, Iran.

Accepted 17 June, 2013

Stepped chute flows are characterized by intense turbulence and strong flow aeration, but most studies did not investigate the turbulence characteristics. In this study, highly turbulent air-water flows skimming down a large-size stepped chute were systematically investigated. An experimental study of detailed air-water flow properties measurements were introduced in different types of flow regimes on a stepped chute (θ = 21.8°, h = 0.04 m, l = 0.10 m) model to investigate the location and the flow depth at inception point of air entrainment and velocity profiles distributions. Detailed velocity and turbulence intensity measurements in flow direction were performed by use of a phase detection conductivity probe which was designed, developed and calibrated by writers. The results showed that the turbulence characteristics vary in different regions. The study showed further that the turbulence intensity increases rapidly close to the step bottom at the viscous sub layer and maximized for 0.4 ≤ y/dc ≤ 0.5 at intermediate region then decreases gradually in the upper region. It is hypothesized that the high turbulence levels in the intermediate region were caused by the continuous deformations and modification of the air-water interfacial structure.

Key words: Air-water flows, conductivity probe, inception point, stepped chute, turbulence intensity.

INTRODUCTION

The interactions between flowing waters and atmosphere may lead to strong air-water mixing and complex multiphase flow situations. The evaluation of the air-water flow properties is particularly important on stepped spillways over RCC dams experiencing moderate unit discharges, because large quantities of air entrain upstream of the spillway toe.

Numerous studies of stepped spillway flows were conducted with different approaches over the past forty years. Studies of spillways with particular focus on stepped chutes include Sorensen (1985), Peyras et al. (1991), Christodoulou (1993), Chamani and Rajaratnam (1999), Chinnarasri and Wongwises (2006), Relvas and Pinheiro (2011), and others. Only a limited number of published papers refer to highly turbulent flows associated with strong free-surface aeration (Chanson and Toombes, 2002; Yasuda and Chanson, 2003).

In civil engineering applications, the flow velocity exceeds typically 5 to 10 m/s, the flow Reynolds number ranges from 1 E+7 to over 1 E+9 in large dam spillways, and free-surface aeration is nearly always observed. Such high-velocity highly-aerated flows cannot be studied analytically or numerically because of the large number of relevant equations and parameters. Current knowledge

*Corresponding author. E-mail: mr.beheshti@ sr.iau.ac.ir.

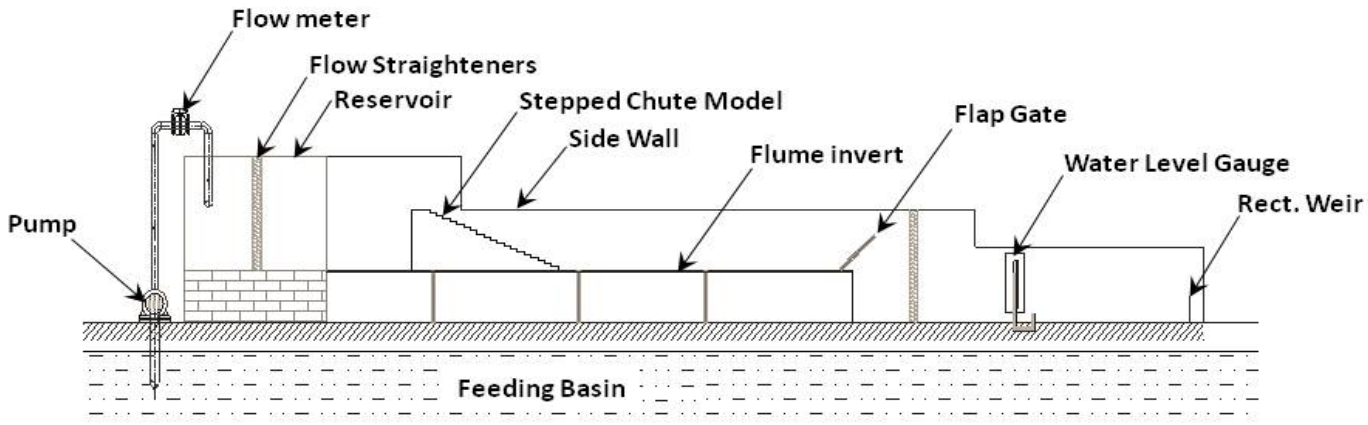

Figure 1. The experimental set-up of the stepped spillway (Hydraulic laboratory of WRI, Tehran, Iran).

relies upon physical modeling and experimental measurements. Accurate measurement systems for air-water flow measurements are limited to intrusive phase-detection probes, hot-film probes, and LDA/PDA systems.

According to the literature review, the measurement of the flow velocity concerns only the longitudinal component, parallel to the mean slope. Double fiber-optical and double-tip conductivity probe are at the moment the more efficient intrusive instrumentation to measure the mixture flow velocity. In fact, the Prandtl tube or back-flushing Pitot tube is limited to low aerated flow (that is, for air concentration less than 0.7).

In the present study, new experiments were conducted in a large stepped channel with a 21.8° slope and it is shown that the advanced developed dual-tip conductivity probe may provide new information on the air-water turbulent characteristics on stepped chutes. Detailed air-water flow properties were recorded systematically for several flow rates including turbulence levels, void fractions and velocity distributions. The results provide a new understanding of the complicated air-water structure on stepped spillways.

MATERIALS AND METHODS

Experimental setup

The experiments were conducted in a rectangular Perspex-walled flume in the Hydraulics laboratory at the water research Institute of Iran Power Ministry. The experimental channel was 5 m long and 0.90 m wide. Water flow was supplied from a large feeding basin under the laboratory leading to a concrete reservoir upstream of the flume.

The test section consisted of a broad crested weir (0.83 m wide, 0.45 m long, with upstream sharped corner) followed by twenty identical steps (h = 0.04 m, l = 0.10 m) made of Plexi-Glass plates. The stepped chute was 0.83 m wide with Perspex sidewalls followed by a horizontal steel-invert flume ending in a dissipation pit (Figure 1). The physical model is part of a closed water cycle.
The chute bottom angle, equal to the pseudo-bottom angle, was φ = 21.8° (1V : 2.5H).

The measurement reach located at 3.5 from the entrance channel section, was 3 m long. A pump controlled with an adjustable frequency AC motor drive delivered the flow rate, enabling an accurate discharge adjustment in a closed-circuit system.

At the downstream end of the flume, the tail gate controls the tail water depth. For all measurements, the gate was fully opened.

Instrumentation and measurement techniques

In present study, the measured parameters are included: clear-water flow depths, clear-water and air-water flow velocities and flow rate.

Clear-water flow depths were measured using a rail mounted vertical pointer gauge with 1 mm accuracy. Clear-water velocities were measured with a Pitot tube (3.3 mm external diameter, 20 mm distance between tip and lateral holes). The flow rate measurements were performed using a rectangular sharp-crested weir located in the outlet channel and an electromagnetic flow meter positioned in the inlet pipe, used for confirmation of the weir discharge measurements. Detailed information about air-water flow properties like the air-water flow velocity, the air concentration and bubble sizes and frequencies was gained using a double-tip conductivity probe (Ø = 0. 7 mm) which was developed and calibrated at Science and Research Branch of Islamic Azad University by authors.

The conductivity probe is a phase-detection intrusive probe designed to pierce the bubbles. The phase-detection relies on the difference in electrical resistance between air and water. The probe mounted on a support frame parallel to the chute slope and consists of two identical tips made of stainless steel surgical needle. The tips are aligned in the flow direction and the distance between the tips is 4 mm (Figure 2). The sampling frequency of the developed probe is 50 kHz with adjustable sampling time. The two-phase flow properties measurements were taken from the tip of the steps to as close to the water surface as possible. All measurements were performed on the channel centerline (z = 0) at step edges and adjacent step edges.

Experimental flow conditions

In the stepped chute, the basic flow regimes were inspected in a series of visual observation with discharges ranging from 0.012 m^3/s to 0.035 m^3/s (Table 1). The model development was based on the Froude similitude. The facility was designed to operate with flow conditions ranging from nappe to skimming flow regimes. The

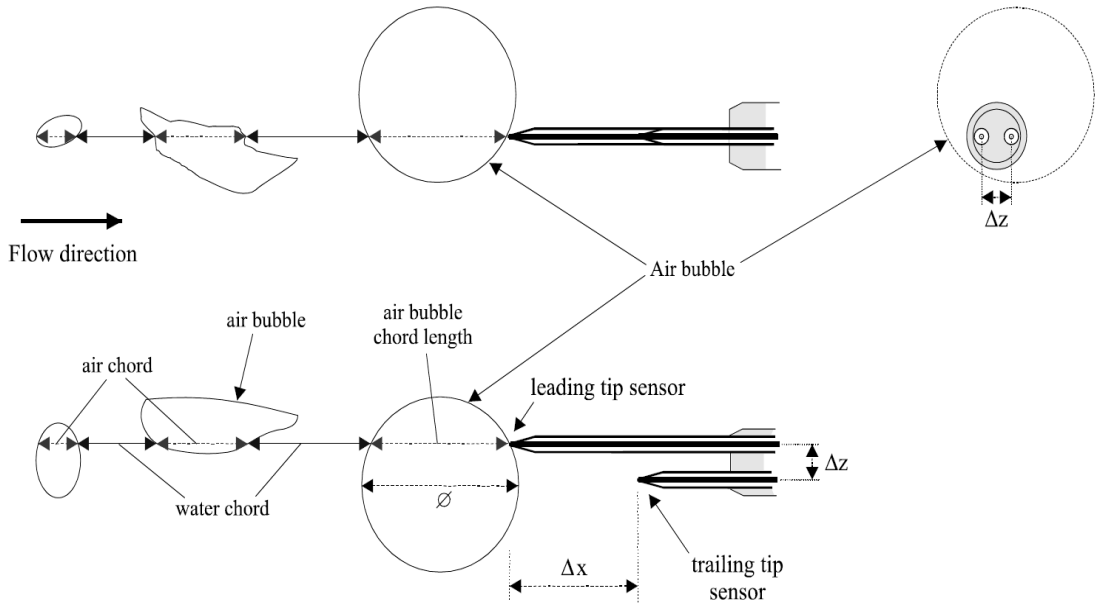

Figure 2. Sketch of the double-tip conductivity probe and its operation.

Table 1. Summary of experimental flow conditions (Present study).

Q_w, m³/s (1)	q_w m³/s/m (2)	d_c/h (3)	Re (4)	We (5)	Flow regime (6)	Location of inception of air entrainment (7)	Remarks (8)
0.012	0.0147	0.701	5.8×10^4	102.519	Nappe Flow	Step edge 4	W = 0.83 m, h = 0.04 m, l = 0.10m
0.015	0.0184	0.813	7.2×10^4	109.975	Transition Flow	Step edge 4	W = 0.83 m, h= 0.04 m, l = 0.10m
0.020	0.0241	0.981	9.6×10^4	119.380	Transition Flow	Step edge 6	W = 0.83 m, h= 0.04 m, l = 0.10m
0.025	0.0301	1.131	1.2×10^5	119.788	Skimming Flow	Step edge 7	W = 0.83 m, h= 0.04 m, l = 0.10m
0.030	0.0361	1.282	1.4×10^5	204.789	Skimming Flow	Step edge 7	W = 0.83 m, h= 0.04 m, l = 0.10m
0.035	0.0422	1.415	1.7×10^5	314.580	Skimming Flow	Step edge 8	W = 0.83 m, h= 0.04 m, l = 0.10m

flow conditions corresponded to flow Reynolds numbers ranging from 5.8×10^4 to 1.7×10^5. The Reynolds number defined in terms of the hydraulic diameter as:

$$R_e = V \times D_H / u_w \quad (1)$$

Where D_H is the hydraulic diameter, V and u_w are the interfacial velocity and the kinematic viscosity of the water, respectively.
The measured flow rates, and other experimental parameters of the different conditions, are shown in Table 1.

Data processing

Air-water flow properties were recorded for nappe (that is, dc/h < 0.701), transition (0.701 < dc/h < 0.1.131) and skimming flows (that is, dc/h > 1.131). In rectangular channels, the critical depth is estimated by $d_c = \sqrt[3]{q_w^2 / g}$ where q_w is the water discharge per unit width and g is the gravity acceleration.

During each test, photographic observations recorded the inception point of air entrainment. The inception point was noted as the location where the flow changed from a glassy, smooth appearance to a more frothy appearance at the free surface. The inception point location was described quantitatively by its horizontal distance from the spillway crest and with regards to step location within the spillway chute. On stepped spillways, the position of the start of air entrainment is a function of the discharge, spillway roughness, and step geometry.

Velocity measurement is based upon the successive detection of air-water interfaces by two tips. This technique assumes that the probe tips are aligned along a streamline and that bubbles and droplets are little affected by the leading tip. When a proportion of bubbles strike the leading tip and trailing tip sequentially, the resulting signals from the two tips will be similar with a slight time delay. This time delay is the average time for a bubble to travel the distance between the two tips. If this distance is known, the time can be converted into a mean air-water interface velocity.
The time-averaged air-water velocity equals:

$$V = \frac{\Delta X}{T} \quad (2)$$

Where Δx is the longitudinal distance between probe sensors (Figure 2) and T is the air-water travel time between the two probe sensors. Air-water flow characteristics data were collected at 50 KHz frequency with a sampling duration of 90 s. The data analyses were done in Excel spread sheets and Grapher V.9.1.536 software.

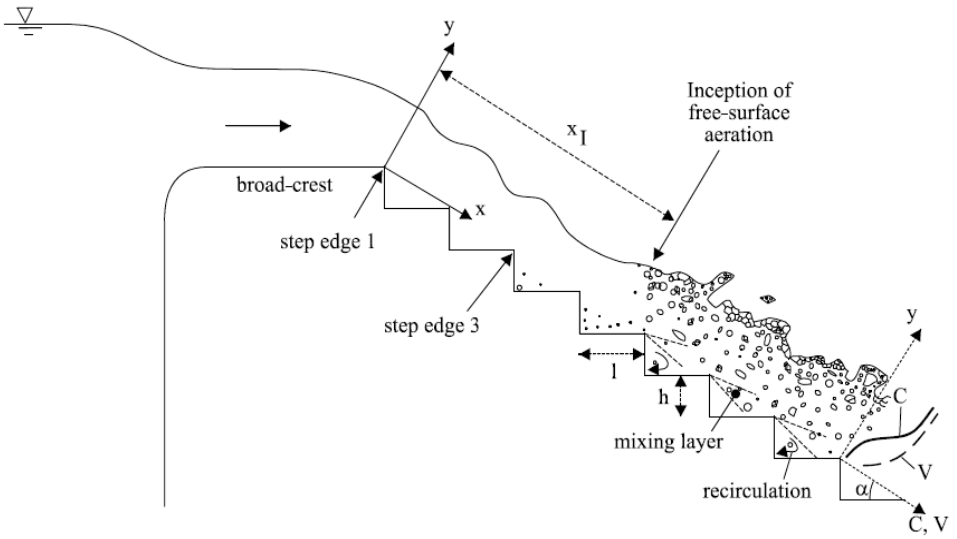

Figure 3. Definition sketch of flow over stepped chute.

In analysis, the distribution of the time averaged velocity, air concentration, fluctuating velocities and turbulence intensities as well as their decay along the downstream direction were considered.

EXPERIMENTAL RESULTS AND DISCUSSION

Detailed measurements of air-water flow properties were conducted for a number of dimensionless flow rates (d_c/h).

The maximum water heads above the spillway crest are between 86.25 and 93.95 cm (measured from the toe of the spillway as the datum) and corresponding unit width discharges between 0.0147 and 0.042 $m^3/s/m$. The approach flow conditions corresponding to Froude numbers between 0.643 and 1.007.

A right hand coordinate system was adopted at measuring sections in the flume with x-axis as the streamwise distance along the channel bottom, y-axis as the distance measured normal to the invert (or channel bed) and z-axis as the transverse distance from the channel centerline.

The dimensionless distributions of interfacial velocity and turbulent intensity showed some characteristic features.

Basic flow observations

Flow regimes

For a given chute geometry, the flow pattern above a stepped channel may be nappe flow, transition flow or skimming flow. The type of flow regime is a function of the discharge and step geometry (Chanson, 1994b; Chanson and Cummings, 1996). For low discharges, the water flow drops from step to step on a stepped chute. That is the nappe flow regime which was studied by Chamani and Rajaratnam (1994), Chanson (1994a), Toombes (2002), El-kamash et al. (2005), and Toombes and Chanson (2008).

For some intermediate discharge, the transition flow regime is observed which is characterized by a chaotic behavior and strong splashing and droplet projections downstream of the inception point of free surface aeration (Chanson, 2001b, Chanson and Toombes 2004). For this regime, the flow can appear as nappe flow (presence of air caity) for some steps and as skimming (onset of vortices in a filled step) for the rest. For larger flows, the waters skim above the pseudo-bottom formed by the step edges.

The skimming flow is characterized by strong cavity recirculation with three-dimensional vortical patterns (Rajaratnam, 1990; Chanson 1994b, 1995a; Chamani and Rajaratnam, 1999). The flow regime changes in the stepped chute was observed and analyzed in this study. The conditions linked to the flow configuration changes have been quantitatively studied. The parameters which have been considered to quantify these changes are the ones related to flow critical depth (dc) and to the spillway geometry, which are the non-dimensional ratios d_c/h and h/l where dc is the critical depth and h and l are the step height and length respectively. A sketch of stepped chute flow and other geometrical parameters are shown in Figure 3.

A nappe flow regime without hydraulic jump was observed for small flow rates ($d_c/h < 0.813$) and for large flow rates ($d_c/h > 1.131$), the water skims over the pseudo-bottom. At moderate discharge rates ($0.813 < d_c/h < 1.131$), a transition flow pattern was observed. The non-dimensional characteristic depth (d_c/h) values corresponding to the different flow regime observations

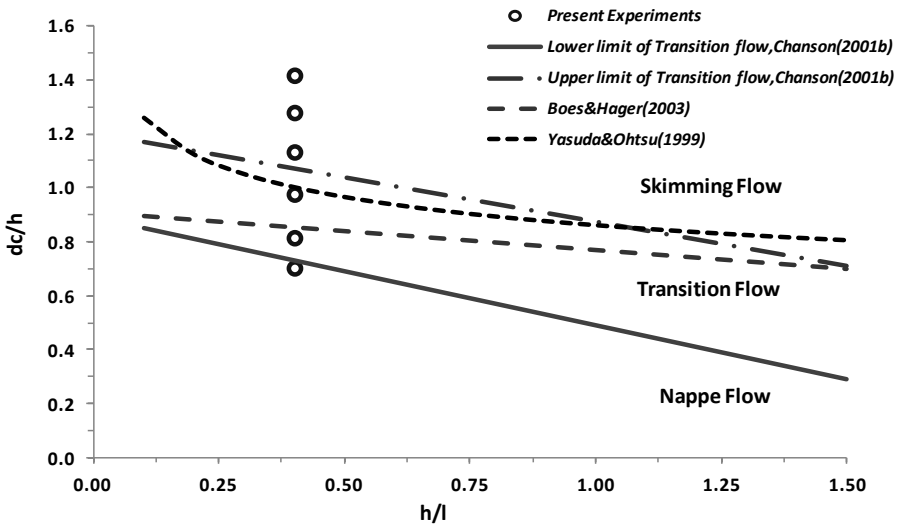

Figure 4. Flow regimes estimation on the stepped chute and comparison with the empirical relationships.

are shown in Figure 4 and compared with some researchers' observations.

The observation results for flow regime prediction were in agreement with onset/transition functions in the literature (Chanson, 1995a, 2001b).

Characterizing the inception point of air entrainment

At the upstream end of the stepped spillway, a turbulent boundary layer is generated by bottom friction and it develops in the flow direction. When the outer edge of the developing boundary layer reaches the vicinity of the free-surface, air entrainment is initiated.

This location is called the inception point of free-surface aeration. Downstream, the turbulence next to the free-surface is large enough to initiate substantial flow aeration. In the present study, the location of the inception point of free-surface aeration was recorded in all flow regimes. At the inception point, the air is entrained into the flow owing to a large degree of turbulence.

Determination of the inception point location along the spillway is important to estimate the unaerated zone, which is prone to the cavitation damage. Cavitation is a serious problem resulting from hydrodynamic pressures, on the step surfaces or at the step edges, which could fall below the vapor pressure (Boes and Hager, 2003).

Cavitation might cause severe damage to the steps and can be mitigated by a significant aeration along the spillway. Prevention of cavitation potential damage requires a mean air concentration of at least 5 to 8% (Peterka, 1953). For all the current models experiments, the location of the inception point was defined by visual observation and pointer gauge measurements of the water surface where the air was entrained into the flow for the whole spillway width. The non-dimensional parameter x_I/k_s, is plotted as a function of the roughness Froude number (Fr*) in Fig. 5 for current experimental data. The parameter k_s is defined as the step roughness height and equals to hcosθ. Fr* is a Froude number defined in terms of the step roughness:

$$F_r* = q_w \Big/ \sqrt{(h\cos\theta)^3 g \sin\theta} \quad (3)$$

The available literature data are also shown in Figure 5 and compared with the current data. Figure 5 shows there are good agreement of the results with Boes and Hager (2003) and a fair agreement with others. For the present study, the results were best correlated by the following equation to locate the inception point of air entrainment on the 21.8° stepped chute for 0.701<dc/h<1.415:

$$\frac{X_I}{K} = 8.0833 \mathrm{E}_*^{0.7723} \quad (4)$$

Interfacial velocity and turbulent intensity distributions

In analogy with the studies of uniform rough flow for steep gravel beds in mountain streams, a few authors (Chamani and Rajaratnam, 1999) suggested that above the pseudo-bottom, the homogeneous air-water flow agrees with the rough boundary layer theory. However, because of the high relative roughness of the steps, the 3D pattern of the macro-turbulence structures as well as

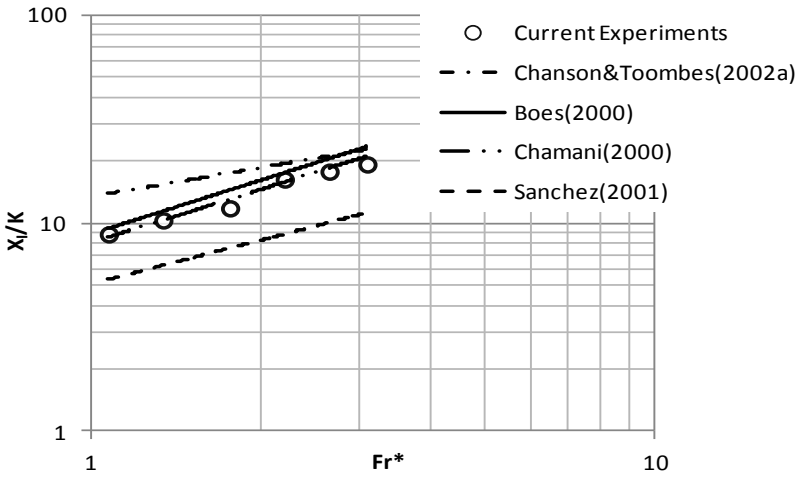

Figure 5. Dimensionless location of the inception point of free-surface aeration.

Table 2. Comparison of the power law coefficients for velocity distribution.

References	D	N	Remarks
Chanson (2001b)	1	5~6	Skimming flow
Chamani and Rajaratnam(1999)	1	6.3	$\theta = 30°$
Boes(2000)	1	6.3	$0.04 \le Y_{90} \le 0.5$
Boes and Hager (2003)	1.05	4.3	$0.04 \le Y_{90} \le 0.8$, $26° \le \theta \le 55°$
Yasuda and Chanson (2003)	1	9	$0.05 \le Y_{90} \le 1$, $\theta = 15.6°$
Current Study	1.012	5.21	$0.03 \le Y_{90} \le 0.92$, $\theta = 21.8°$

the drag around steps, the classical logarithmic equation as proposed by Karman-Prandtl is not fully applicable.

$$\frac{v(x)}{\sqrt{\tau_o / \rho_w}} = \frac{2.30}{\kappa} \log\left(\frac{x}{\kappa}\right) + C1 \quad (5)$$

In which k is the von Karman turbulence constant determined experimentally between 0.40 and 0.42,
C1 an integration constant, k the equivalent roughness size and τ_0 the boundary shear stress.

Nevertheless, most researchers proposed that above the pseudo-bottom the local mixture velocity depends on the maximum velocity and that the velocity distribution follows a power law given by:

$$U_{90} = DY_{90}^{1/N} \quad (6)$$

Where $U_{90} = \frac{u}{u_{90}}$ and $Y_{90} = \frac{y}{y_{90}}$ are the dimensionless mixture flow velocity and depth respectively. u_{90} and y_{90} are the velocity and flow depth corresponding to 90% air concentration. D and N are coefficients obtained from experiments data. This result has been validated for model and prototype data of air-water open channel flows by several other researchers, including Chanson (1989), Wood (1991) and Chanson and Cummings (1996). However, depending on the tested discharges or the portion of flow layer considered in the empirical fitting, several power laws have been proposed with different coefficients and some of them were listed in Table 2.

In the present study, the velocity power law exponent was 1/5.21 in average (that is, N = 5.21), although it varied between adjacent step edges. Such fluctuations were believed to be caused by some interference between adjacent shear layers and cavity flows. In current study, the velocity distributions at each step edge compared favorably with the power-law function for $y/y_{90} < 1$ and with a uniform profile for $y/y_{90} > 1$:

$$\left(\frac{u}{u_{90}}\right) = D\left(\frac{y}{y_{90}}\right)^{1/N}, \quad 0 \le \frac{y}{y_{90}} \le 1 \quad (7)$$

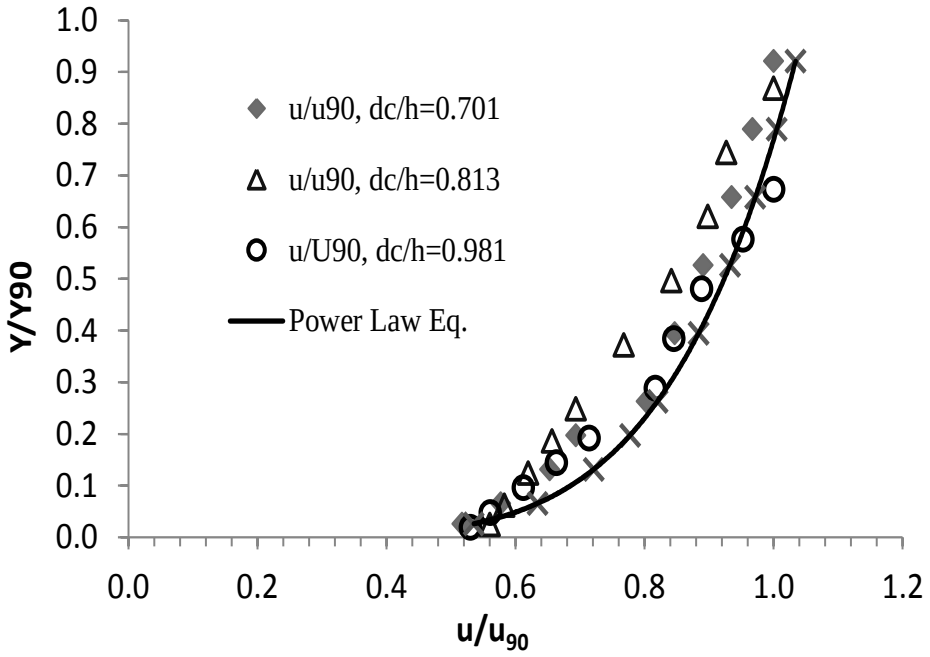

Figure 6. Dimensionless distributions of normalized interfacial velocity u/umax in different flow regimes at step edge 15.

$$\left(\frac{u}{u_{90}}\right)=1 \ , \quad 1\le\frac{y}{y_{90}}\le 2.5 \tag{8}$$

Equation (7) is compared with experimental data in Figure 6 for several dimensionless discharges dc/h. The data does not include the profiles closest to the sidewall, which are likely affected by sidewall friction. In nappe and transition flows, the velocity measurements show quasi-uniform velocity profiles at step edges (Figure 6).

The result is relatively close to that of Chanson and Toombes (2002). It has no theoretical justification and it is only a rough correlation. The velocity distribution results in skimming flows are basically identical to measured velocity distributions in self-aerated flows on smooth-invert chutes (Cain, 1978), although the rate of energy dissipation is much greater on a stepped cascade and flow resistance is dominated by form drag.

Due to turbulent eddies; the local instantaneous flow velocity (u) within the boundary layer will fluctuate in a more or less random fashion. However, the velocity record for turbulent flow includes both a mean and a turbulent component.

The decomposition of the flow velocity is as follow:

$$u=\bar{u}+u' \quad \rightarrow \quad u'=u-\bar{u} \tag{9}$$

This is commonly called a Reynolds' decomposition, where:

$\bar{u}=$ Time-averaged velocity which equals to $\lim_{T\to\infty}\frac{1}{T}\int_0^T u(t)dt$

$u'=$ Velocity fluctuation in the stream-wise direction also called as characteristic turbulent velocity.

T= sampling time

Two methods are used to describe the turbulence of the flow; single point observations and correlations between multiple points. The more common method uses measurements of velocity fluctuations at one point in the flow. So, an accurate measure of the turbulent intensity can be obtained.

Herein, the turbulent intensity is defined in terms of the statistical quantities which describe the random fluctuations. A convenient measure of the fluctuating component of the flow velocity is the root-mean-square value as below:

$$u'_{rms}=\sqrt{\overline{u'^2}}=\sqrt{\frac{\sum_{i=1}^{n}\left(u_i-\bar{u}\right)^2}{n}} \tag{10}$$

Where n is the number of samples.

The normalized turbulence intensity in flows over a spillway dam is subject to the influence of flow patterns of the boundary layers as well as boundary conditions of different sections (e.g. the dam crest, downstream slope, surface roughness). Turbulence Intensity is a dimensionless measure of the turbulent fluctuations of

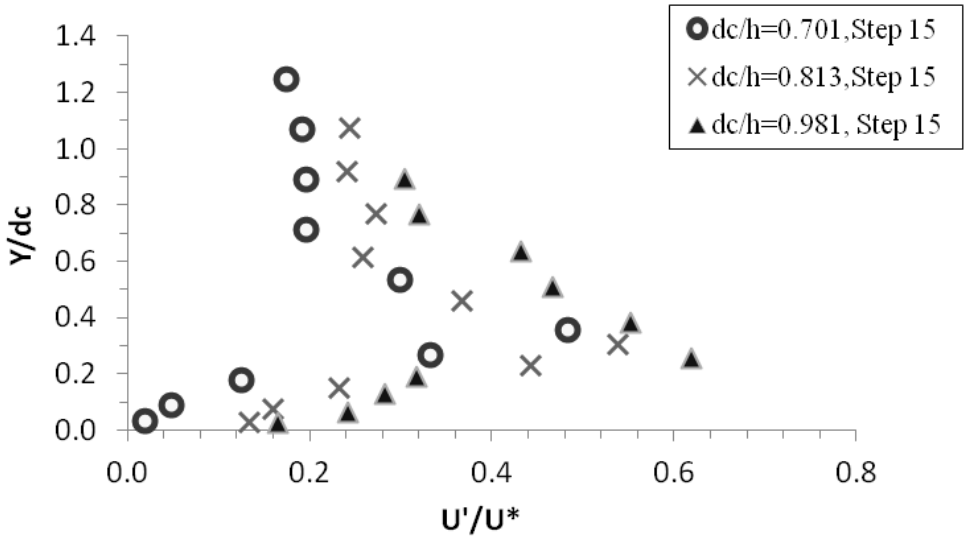

Figure 7. Vertical distribution of turbulence intensity in air-water flow over steps.

interfacial velocity which characterizing turbulence and defined as the root-mean-square value of the fluctuations in the flow direction divided by the shear velocity.

$$T_U = \frac{u'_{rms}}{u*} \quad (11)$$

Where the u* is the shear or friction velocity and can be determined from the boundary shear stress distribution based upon the friction slope S_f, if the flow is gradually varied.

The shear velocity have a great impact on the distribution of the mean velocity and turbulence structure in the boundary layer and is the most fundamental velocity scale with which to normalize mean velocity and turbulence.

$$u* = \sqrt{\tau_o / \rho_w} \quad (12)$$

$$\tau_0 = g\rho_w S_f \int_{y=0}^{y=y_{90}} (1-C)dy \quad (13)$$

Where the frictions slope $S_f = -\frac{\partial H}{\partial x}$ is the slope of the total head line.

Figure 7 shows the normalized turbulent intensities (Tu) distributions at different verticals and relative discharges (d_c/h). The data were obtained at step edges and at the same dimensionless distance from the inception point.

It can be seen from Figure 6 that the turbulence characteristics vary in different regions. Herein, the turbulence intensity increases rapidly close to the step bottom at the viscous sub layer and maximized for 0.4≤ y/dc ≤ 0.5 at intermediate region then decreases gradually in the upper region. A similar trend was observed in previous studies (Chanson and Toombes, 2002; Gonzalez, 2005; Chanson and Carosi, 2007a). It is hypothesized that the high turbulence levels in this intermediate region were caused by the continuous deformations and modification of the air-water interfacial structure.

Conclusions

Flows cascading down a stepped spillway with a moderate slope are characterized by some strong aeration and high turbulence of the flow. In this study, a set of air-water flow experiments were preformed in high velocity flows on a relatively large stepped channel based on Froude similitude.

The two phase flow measurements were preformed with a conductivity double-tip probe downstream of the inception point of aeration. The results included air water flow properties such as air concentration, flow velocity, turbulence, and bubble count rate. Based on measured air-water velocities, the flow shear stress, friction velocity and turbulence intensities were estimated accurately. The air-water flow properties presented some basic characteristics that were qualitatively and quantitatively in agreement with previous studies. High turbulence levels were recorded downstream of the aeration inception point. The distributions of turbulence intensity had a similar shape as clear-water flow data of Ohtsu and Yasuda down a stepped chute.

The measurements showed that immediately downstream of the inception point of air entrainment, the flow is rapidly varied and the maximum turbulence intensities occurred in the intermediate region between the spray and bubbly flow regions (that is, 0.3 < C < 0.7).

Although the findings were obtained for a moderate slopes (θ = 21.8°), it is believed that the outcomes are valid for a wider range of chute geometry and flow conditions typical of embankment chutes.

ACKNOWLEDGEMENT

The funding for these and related studies was provided by the Guilan Regional Water Company. Also, the authors acknowledge the helpful discussion with Prof. Chanson and Mr. Reza Rushan (Head of Hydraulics structures Department of the Water Research Institute, Power Ministry, Tehran, Iran).

Nomenclature: C, Void fraction defined as the volume of air per unit volume; **DH,** hydraulic diameter (m); **d,** characteristic depth (m); **dc**, critical flow depth (m); **Fr*,** Froude number defined in terms of the roughness height; **H,** total head (m); **Hmax,** maximum head available (m) using the spillway toe as datum; **H,** height of steps (m) (measured vertically); **ks,** step dimension (m) measured normal to the flow direction; **l,** length of steps (m) (measured horizontally); **Qw,** water discharge (m^3/s); **qw,** water discharge per unit width (m^2/s); **Re,** Reynolds number defined in terms of the depth-averaged flow velocity and **Sf,** hydraulic diameter friction slope; **T,** sampling time(s); **Tu,** turbulence intensity; **Uw,** equivalent clear-water flow velocity (m/s); **u',** root mean square of longitudinal component of turbulent velocity (m/s); $\bar{u}$, time-averaged velocity(m/s); **u*,** shear or friction velocity(m/s); **W,** stepped spillway width (m); **we,** Weber number; **x,** longitudinal/streamwise distance (m); **xI,** distance (m) from the start of growth of boundary layer to the inception point of air entrainment; **y,** distance (m) from the pseudo-bottom (formed by the step edges) measured perpendicular to the flow direction; y_{90}, characteristic depth (m) where the air concentration is 90%; τ_0, boundary shear stress (Pa).

Subscripts: c, Critical flow conditions; **f,** friction; **I,** characteristics of the inception point; **l,** a discrete point; **max,** maximum value in a cross-section; **rms,** root mean square; **w,** water flow; **90,** flow conditions where C = 0.90.

REFERENCES

Boes M (2000). Role of natural and immune IgM antibodies in immune responses. Mol. Immunol. 37:1141–1149.

Boes RM, Hager WH (2003). Hydraulic Design of Stepped Spillways. J. Hydr. Eng. pp. 671-679.

Chamani MR, Rajaratnam N (1994). Jet Flow on Stepped Spillways. J. Hydr. Eng. A.S.C.E. 120(2):254-259.

Chamani MR, Rajaratnam N (1999). Characteristics of Skimming Flow over Stepped Spillways., J. Hydr. Eng. ASCE. 125(4):361-368.

Chanson H (1989). Study of Air Entrainment and Aeration Devices. J. Hydr. Res. IAHR. 27(3):301-319.

Chanson H (1994a) "Hydraulic Design of Stepped Cascades, Channels, Weirs and Spillways, Pergamon, Oxford, UK, Jan. P.292 (ISBN 0-08-041918-6).

Chanson H (1994b). Hydraulics of Skimming Flows over Stepped Channels and Spillways, J. Hydr. Res. 32:445-460

Chanson H (1995a). Hydraulic Design of Stepped Cascades, Channels, weirs and Spillways, Pergamon, Oxford, UK.

Chanson H (2001b). A Transition Flow Regime on Stepped Spillways? The Facts. In Proceedings of the 29th IAHR Biennial Congress, Beijing, China, Theme D. Vol.1. Edited by G. LI.Tsinghuna University Press, Beijing, pp.490-498.

Chanson H, Cummings PD (1996). Air-Water Interface Area in Supercritical Flows down Small-Slope Chutes. Research Report No. CE151, Dept of Civil Engineering, University of Queensland, Australia, P. 60.

Chanson H, Toombes L (2002). Air-Water Flows down Stepped Chutes: Turbulence and Flown Structure Observations. Int. J. Multiphase Flow. 28(11):1737-1761.

Chanson H, Toombes L (2004). Hydraulics of Stepped Chutes: the transition flow. J. Hydr. Res. 42:43-54.

Chanson H, Carosi G (2007a). Advanced post-processing and correlation analyses in high-velocity air–water flows. Springer, J. Environ. Fluid Mechanics, 7:495–508.

Chinnarasri C, Wongwises S (2006). Flow patterns and energy dissipation over various stepped chutes, J. Irrig. Drain. Eng. 132(1):70–76.

Christodoulou GC (1993). Energy Dissipation on Stepped Spillways, J. Hydr. Eng. A.S.C.E. 19(5):644-650.

El-Kamash MK, Loewen MR, Rajaratnam N (2005). An Experimental Investigation of jet flow on a stepped chute, J. Hydr. Res. 43:31-43.

Gonzalez CA (2005). An Experimental Study of Free-Surface Aeration on Embankment Stepped Chutes, Ph.D. Thesis, Department of Civil Engineering, The University of Queensland, Brisbane, Australia, P.240.

Peterka AJ (1953). The effect of entrained air on cavitation pitting, Joint Meeting Paper, IAHR/ASCE, Minneapolis, Minnesota, Aug.

Peyras L, Royet P, Degoutte G (1991). Ecoulement et Dissipation sur les Déversoirs en Gradins de Gabion (Flow and Energy Dissipation of Energy on Gabion Weirs), La Houille Blanche, 1:37-47.

Rajaratnam N (1990). Skimming Flow in Stepped Spillways. J. Hydr. Eng. 116(4):587-591.

Relvas AT, Pinheiro AN (2011). Stepped chutes lined with wedge-shaped concrete blocks: Hydrodynamic pressures on blocks and stability analysis, Can. J. Civ. Eng. 38(3):338–349.

Sorensen RM (1985). Stepped Spillway Hydraulic Model Investigation, J. Hydr. Eng. ASCE. 11(12):1461-1472.

Toombes L (2002). Experimental Study of Air-Water Flow Properties on Low-gradient Stepped Cascades. Ph.D. thesis, Dept of Civil Engineering, University of Queensland, Brisbane, Australia.

Toombes L, Chanson H (2008). Flow patterns in nappe flow regime down low gradient stepped chutes, J. Hydr. Res. 46(1):4–14.

Wood IR (1991). Air Entrainment in Free-Surface Flows, IAHR Hydraulic Structures Design Manual, No. 4, Hydraulic Design Considerations, Balkema Publ., Rotterdam, The Netherlands, P.149.

Yasuda Y, Chanson H (2003). Micro -and Macro-Scopic study of two-phase flow on a stepped chute, Proc. XXX IAHR Congress, Thessaloniki, Greece, 695-703.